

11,10

Van der Waals encapsulation of carbon nanotubes

© A.V. Savin^{1,2}, O.I. Savina²

¹ N.N. Semenov Federal Research Center of Chemical Physics, Russian Academy of Sciences, Moscow, Russia

² Plekhanov Russian University of Economic, Moscow, Russia

E-mail: asavin00@gmail.com, asavin@chph.ras.ru

Received February 18, 2025

Revised February 21, 2025

Accepted February 23, 2025

Encapsulated carbon nanotubes lying on a flat substrate have been modeled. It is shown that encapsulation of nanotubes (coating with a sheet of graphene or hexagonal boron nitride) promotes their collapse. Coating the nanotube with the sheet leads to the appearance of effective (internal) pressure on its surface, which in some areas can reach maximum values of 8 GPa. The average value of the internal pressure monotonically decreases with increasing nanotube diameter (doubling of the diameter leads to more than twofold decrease of the pressure). It is shown that inside the encapsulated nanotube cluster the pressure is uniformly distributed. For a nanotube cluster with a chirality index (5,0), the internal pressure can reach 2 GPa. Encapsulation can increase the interaction energy of nanotubes more than ten times. Combining two encapsulations allows an energy gain of 1.22 eV, but bringing them closer together requires overcoming an energy barrier of 0.14 eV (encapsulations attract at short distances and repel at long distances). Covering the nanotube cluster with a sheet of graphene significantly increases its stability. The molecular dynamics method shows that the encapsulated cluster retains its crystalline structure at $T < 500$ K, and at higher temperatures its melting occurs, accompanied by a significant increase in the volume of the interlayer cavity (pocket) in which it is located. The cavity takes the form of a semicircle, and its volume increases monotonically with increasing temperature.

Keywords: carbon nanotubes, graphene, van der Waals encapsulation.

DOI: 10.61011/PSS.2025.03.60887.36-25

Introduction

Carbon atoms can create numerous structures, among which graphene, a monatomic crystalline layer, has recently received much attention in the research community [1–5]. This nanomaterial is of interest due to its unique electronic [6], stress-strain [7] and thermal properties [8,9].

Strong focus is made on other graphene-like materials such as hexagonal boron nitride (h-BN), fluorographene (CF), molybdenum disulfide MoS₂, tungsten selenide WSe₂ sheets. These two-dimensional materials offer wide opportunities for creating heterostructures in the form of Van der Waals stacks having new properties [10–13]. An important feature of such heterostructures is their ability to hold molecules in localized regions between adjacent layers. Due to the Van der Waals interaction between layers, internal pressure in the order of several GPa might occur in such traps (nanopockets) [14–16], which may alter the properties of the trapped material considerably. Covering of a molecular system with a graphene sheet (Van der Waals encapsulation) is a convenient way to create high local pressure for modifying the system properties [17] or for system storage [18,19].

High pressure induced by the Van der Waals encapsulation may cause collapsing of carbon nanotubes [16]. This study will simulate the behavior of an encapsulated carbon nanotube cluster. Dependence of the internal

pressure on the size and number of nanotubes will be obtained, interaction between the encapsulated nanotubes will be described and encapsulated cluster melting will be simulated. Section 2 describes the model to be used. Section 3 simulates the encapsulated nanotube collapse and reviews internal pressure distribution. Section 4 describes internal pressure distribution within the encapsulated nanotube cluster. Interaction between encapsulated nanotubes is simulated in Section 5. Encapsulated cluster behavior is simulated in Section 6. Finally (Section 7), the main findings are provided.

1. 2D model

To describe the behavior of laminar structures made of graphene (G), hexagonal boron nitride (h-BN) sheets, nanotubes and nanoribbons, it is convenient to use a two-dimensional molecular chain system model [20–23]. Assuming that G and h-BN nanosheets and nanotubes lie in such a way that the zigzag direction of all of them coincides with the x (Figure 1), then the two-dimensional chain model will describe the multilayer system cross-section along this axis. In this model, all nanoribbon (nanotube) atoms with the same coordinates x, z correspond to a single particle.

If atoms along the same line parallel to the y axis move synchronously and only the x and z coordinates

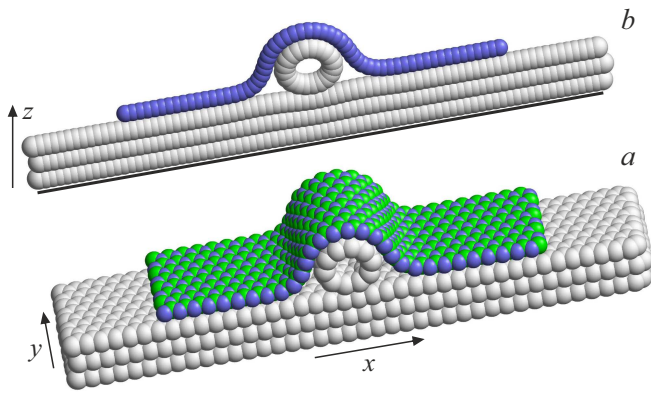


Figure 1. Two-dimensional chain modelling scheme for simulating a carbon nanotube placed on a flat crystalline graphite surface and covered by a hexagonal boron nitride sheet: *a* — full-atomic model, *b* — two-dimensional chain model (black line shows a fixed flat substrate).

are changed, then the Hamiltonian of one G and h-BN nanoribbon will have the form of a Hamiltonian of a chain in the xz plane:

$$H_i = \sum_{n=1}^N \left[\frac{1}{2} M_i (\dot{\mathbf{u}}_n, \dot{\mathbf{u}}_n) + V_i(r_n) + U_i(\theta_n) + Z(\mathbf{u}_n) \right]. \quad (1)$$

Here, $i = 1, 2$ for the G, h-BN nanoribbon. Two-dimensional vector $\mathbf{u}_n = (x_n, z_n)$ sets the coordinates of the n -th particle of the chain. The particle mass link for the G chain coincides with the atomic mass of carbon $M_1 = M_C = 12m_p$, and for the h-BN chain coincides with the average mass of boron and nitride $M_2 = (M_B + M_N)/2 = 12.4085m_p$ ($m_p = 1.66 \cdot 10^{-27}$ kg is the proton mass).

Potential

$$V_i(r) = \frac{1}{2} K_i (r - a_i)^2 \quad (2)$$

describes the longitudinal chain stiffness, K_i is the interaction stiffness, a_i is the equilibrium bond length (chain pitch), $r_n = |\mathbf{u}_{n+1} - \mathbf{u}_n|$ is the distance between the adjacent particles n and $n + 1$.

Potential

$$U_i(\theta) = \epsilon_i [1 + \cos(\theta)] \quad (3)$$

describes the bending stiffness of the chain, θ is the angle between two adjacent bonds,

$$\cos(\theta_n) = -(\mathbf{v}_{n-1}, \mathbf{v}_n) / r_{n-1} r_n,$$

vector $\mathbf{v}_n = \mathbf{u}_{n+1} - \mathbf{u}_n$.

The parameters of potentials (2), (3) for the G chain are determined in [20,21] from the analysis of the dispersion curves of a graphene nanoribbon: longitudinal stiffness $K_1 = 405$ N/m, chain pitch $a_1 = r_{CC} \sqrt{3}/2 = 1.228$ Å ($r_{CC} = 1.418$ Å — C–C valence bond length in the graphene sheet), energy $\epsilon_1 = 3.5$ eV. For the h-BN

chain, parameters of these potentials are determined in [23]: longitudinal stiffness $K_2 = 480$ N/m, chain pitch $a_2 = r_{BN} \sqrt{3}/2 = 1.252$ Å ($r_{BN} = 1.446$ Å — B–N valence bond length in the h-BN sheet), energy $\epsilon_2 = 1.10$ eV.

Chain Hamiltonian (1) gives the nanoribbon strain energy falling within a longitudinal band with width $\Delta y = a_i \sqrt{3}$, therefore, if the chain system energy is further normalized to the graphene nanoribbon, then the h-BN nanoribbon energy shall be multiplied by the normalization factor $c = a_1/a_2 = r_{CC}/r_{BN} = 0.9808$.

The number of layers shall be limited for simulating the multilayer substrate (graphite crystal surface) behavior. Therefore, it will be assumed that the first (lowest) substrate layer interacts with the fixed flat surface of the crystal (in Figure 1, this surface is shown by a black line). Interaction between the layer atoms and the fixed substrate can be described with a good accuracy by the Lennard–Jones potential (k, l)

$$Z(\mathbf{u}) = Z(z) = \epsilon_0 [k(h_0/z)^l - l(h_0/z)^k] / (l - k), \quad (4)$$

where z is the distance from the chain link to the substrate plane $z = 0$, ϵ_0 is the interaction energy (adhesion energy), h_0 is the equilibrium distance, degrees $l = 10, k = 3.75$. For the graphite crystal $\epsilon_0 = 0.0518$ eV, $h_0 = 3.37$ Å [22,24].

Non-valence (Van der Waals) interactions of chain links can be described with a high accuracy by the Lennard–Jones potential (5,11)

$$W_i(r) = \epsilon_i [5(r_i/r)^{11} - 11(r_i/r)^5] / 6, \quad (5)$$

where r is the distance between the interacting chain links, ϵ_i is the interaction energy, r_i is the equilibrium length. For the interaction between the G chains ($i = 1$), $\epsilon_1 = 0.00832$ eV, $r_1 = 3.607$ Å [22]; for the interaction between the G and h-BN chains ($i = 2$) $\epsilon_2 = 0.014334$ eV, $r_2 = 3.701$ Å [23].

It is sufficient to consider the interaction with the fixed substrate (presence of $Z(\mathbf{u})$) in chain Hamiltonian (1) only for chain describing the upper substrate layers. For these chains, periodic boundary conditions with a period equal to the chain length Na_1 will be used. A free edge condition will be used for a chain describing a sheet that covers the top of nanotube.

A cyclic chain of $N = 2m$ links with the following Hamiltonian corresponds to a carbon nanotube with the chirality index ($m, 0$)

$$H = \sum_{n=1}^N \left[\frac{1}{2} M_1 (\dot{\mathbf{u}}_n, \dot{\mathbf{u}}_n) + V_1(r_n) + U_1(\theta_n) + \frac{1}{2} \sum_{|k-n|>5} W_1(r_{n,k}) \right]. \quad (6)$$

Let's consider a molecular system consisting of l_1 -layer graphene substrate, of l_2 carbon nanotubes lying on this substrate, and of l_3 -layer graphene sheet or hexagonal boron

nitride covering the top of nanotube and the substrate. Hamiltonian of the molecular system will be written as

$$H = \sum_{j=1}^l \sum_{n=1}^{N_j} \frac{1}{2} M_j(\mathbf{u}_{n,j}, \dot{\mathbf{u}}_{n,j}) + E, \quad (7)$$

where $l = l_1 + l_2 + l_3$ is the total number of chains, N_j is the number of particles in the j -th chain, $\mathbf{u}_{n,j} = (x_{n,j}, z_{n,j})$ is the vector that sets positions of the n -th particle of the j -th chain. $M_j = M_1$ for the first $l_1 + l_2$ chains, and for the following chains $M_j = M_1$ and cM_2 for the G and h-BN chains.

Potential energy of the molecular system consists of four parts

$$E = E_1 + E_2 + E_3 + E_4. \quad (8)$$

The first part

$$E_1 = \sum_{j=1}^{l_1} \sum_{n=1}^{N_j} \left[V_1(r_{n,j}) + U_1(\theta_{n,j}) + Z(\mathbf{u}_{n,j}) \right] \quad (9)$$

corresponds to the energy of l_1 G chains that form a sliding substrate of the molecular system. These chains have the same length ($\{N_j = N_s\}_{j=1}^{l_1}$), $r_{n,j} = |\mathbf{v}_{n,j}|$, $\mathbf{v}_{n,j} = \mathbf{u}_{n+1,j} - \mathbf{u}_{n,j}$, angle $\theta_{n,j}$ is determined from equation $\cos(\theta_{n,j}) = -(\mathbf{v}_{n-1,j}, \mathbf{v}_{n,j})/r_{n-1,j}r_{n,j}$.

The second part

$$E_2 = \sum_{j=l_1+1}^{l_1+l_2} \sum_{n=1}^{N_j} \left[V_1(r_{n,j}) + U_1(\theta_{n,j}) + \frac{1}{2} \sum_{|k-n|>5} W_1(r_{n,j;k,j}) \right] \quad (10)$$

sets the energy l_2 of cyclic chains corresponding to carbon nanotubes ($m, 0$) lying on the sliding substrate ($\{N_j = N_n\}_{j=l_1+1}^{l_1+l_2}$, $N_n = 2m$).

The third part

$$E_3 = c_i \sum_{j=l_1+l_2+1}^l \sum_{n=1}^{N_j} \left[V_i(r_{n,j}) + U_i(\theta_{n,j}) \right] \quad (11)$$

sets the energy of the last l_3 chains corresponding to G or h-BN sheets covering the top of nanotubes, $\{N_j = N_c\}_{j=l_1+l_2+1}^l$. Here, $i = 1$, if the G sheet is simulated, and $i = 2$, if the h-BN sheet is simulated ($c_1 = 1$, $c_2 = c$).

The last part describes the interchain interaction energy

$$E_4 = \sum_{j_1=1}^{l-1} \sum_{j_2=j_1+1}^l \sum_{n=1}^{N_{j_1}} \sum_{k=1}^{N_{j_2}} W_i(r_{n,j_1;k,j_2}), \quad (12)$$

where $i = 1$ for the interaction between the G chains and $i = 2$ for the interaction between the G and h-BN chains, $r_{n,j_1;k,j_2} = |\mathbf{u}_{n,j_1} - \mathbf{u}_{k,j_2}|$.

2. Encapsulated nanotube collapse

Let's consider first one carbon nanotube ($m, 0$) lying on a multilayer substrate and covered with a top graphene or

hexagonal boron nitride sheet (Figure 1). For this, a three-layer substrate consisting of G chains ($l_1 = 3$, $N_s = 400$) is used, one cyclic chain ($l_2 = 1$, $N_n = 2m$) is placed above its center and a single-layer or multilayer ($l_3 = 1, 2, 3$, $N_c = 300$) G or h-BN chain is placed on top of the whole structure.

To find a stable steady state of this multilayer system, a potential energy minimum problem shall be solved

$$E \rightarrow \min : \{\mathbf{u}_{n,j}\}_{n=1, j=1}^{N_j, l} \quad (13)$$

with periodic boundary conditions for the first l_1 chains. Problem (13) was solved numerically by the conjugate gradient method. By choosing the minimization procedure starting point, all stable steady states of the multilayer structure may be obtained. The view of steady states of a nanotube with a single-layer cover is shown in Figure 2 and with a two-layer cover is shown in Figure 3.

A nanotube in such system may have two main steady states — open and collapsed. In the open state, small-radius nanotubes are almost round and large-radius nanotubes have a shape of a convex drop lying on a flat surface. The collapsed state has a shape of a nonsymmetric dumbbell where the opposite nanotube surfaces are closely adjacent to each other (Figures 2, *e* and 3, *e*). The open state of the nanotube exists for all values of $m \geq 5$, the collapsed state exists only when the threshold value $m \geq m_1$ is exceeded. The threshold value of the index depends on the type covering sheet and the number of layers. When there is no cover ($l_3 = 0$), $m_1 = 31$, for single-layer, two-layer and three-layer G sheet cover ($l_3 = 1, 2, 3$), $m_1 = 40$, and for the h-BN sheet cover, $m_1 = 33$.

Dependence of the normalized energy E/N ($N = l_1N_s + l_2N_n + l_3N_c$ — the total number of particles) on the nanotube index m is shown in Figure 4. Near m_1 , the open state is always more energetically favorable. As m increases, the difference of energies between the collapsed and open states decreases monotonously. There is the second threshold value of m_2 , when $m \geq m_2$, the collapsed state becomes more energetically favorable (the energy gain is provided by the Van der Waals interaction between the adjacent nanotube surface areas). When there is no cover, $m_2 = 56$, for single-layer, two-layer and three-layer G sheet cover, $m_2 = 52, 50$ and 49 , and for the h-BN sheet cover, $m_2 = 48$.

Thus, encapsulation of nanotubes facilitates nanotube collapsing. Actually, the collapsed state for an uncovered nanotube will be more energetically favorable only for zigzag nanotubes with $m \geq 56$ (for nanotubes with $D > 4.38$ nm), and for a nanotube covered with the h-BN sheet — with $m \geq 48$ ($D > 3.75$ nm). Therefore, encapsulation shall result in collapsing of a part of nanotubes. This explains the experimentally found collapse of some nanotubes during encapsulation [16].

3. Pressure within the encapsulated nanotube system

Change of the encapsulated nanotube shape as the nanotube size increases is shown in Figures 2 and 3. Volume of a nanotube is defined by the cross-section area S (area of a polygon formed by a cyclic chain $\{\mathbf{u}_{n,l_1+1}\}_{n=1}^{2m}$). Dependence of \sqrt{S} on m is shown in Figure 5. The figure shows that a graphene sheet cover always leads to a decrease in the nanotube volume. Nanotube compression coefficient $k = S_{l_3}/S_0$, where S_{l_3} is the cross-section area of a steady state of a nanotube covered by the l_3 -layer graphene sheet, and S_0 is the cross-section area for an uncovered nanotube (with $l_3 = 0$).

Values of k for the open states of a nanotube $(m, 0)$ covered by the l_3 -layer graphene sheet are listed in Table 1. As shown in Figure 5 and Table 1, nanotube compression increases monotonously with increasing size and number of

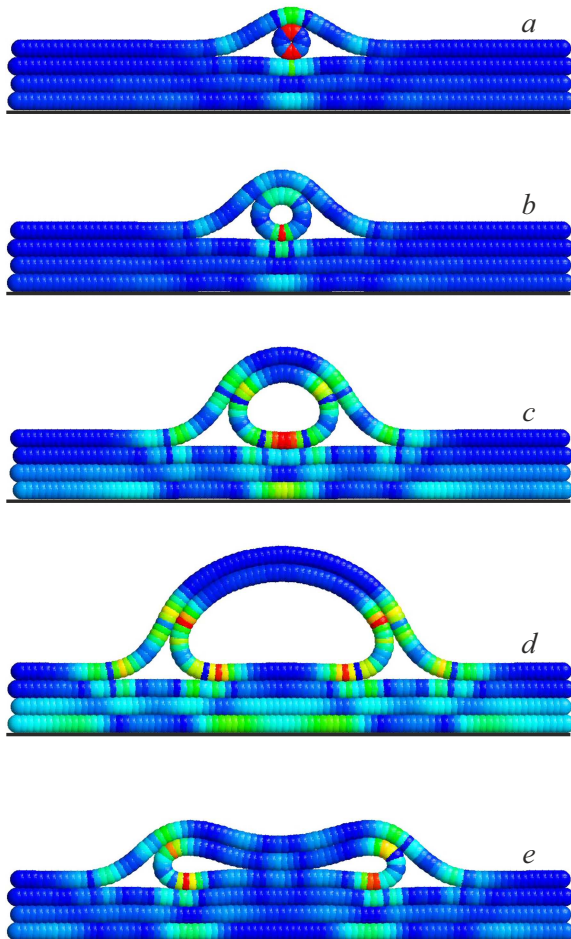


Figure 2. Steady state of the carbon nanotube $(m, 0)$, placed on a multilayer substrate and covered with a single-layer graphene sheet. Internal pressure distribution is shown by different colors, blue — zero pressure, red — maximum pressure P_{\max} . Parts (a–d) show the open state of a nanotube with $m = 5, 10, 20, 40$ ($P_{\max} = 8.0, 8.1, 3.1, 2.1$ GPa), part (e) shows the collapsed state of a nanotube $(40,0)$ ($P_{\max} = 4.5$ GPa).

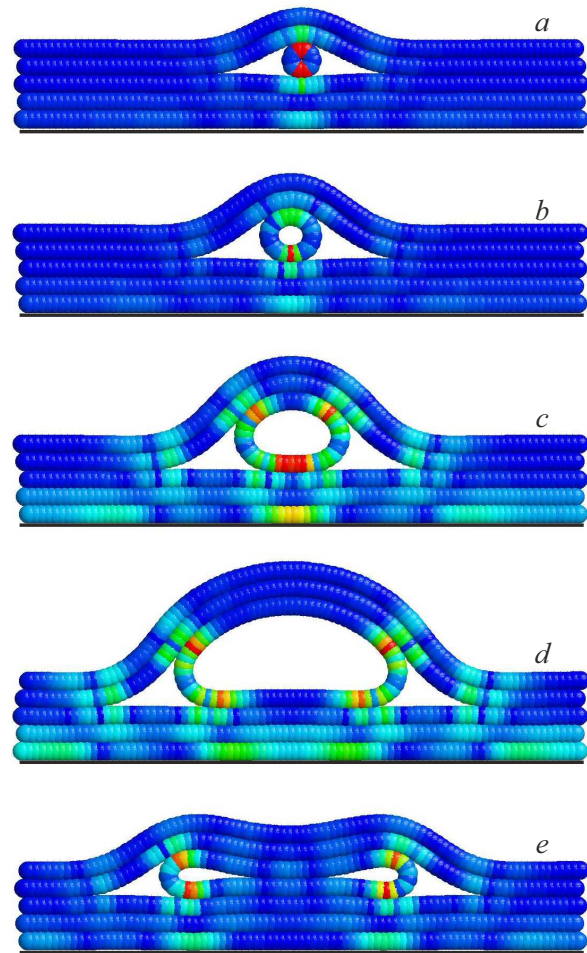


Figure 3. Steady state of the carbon nanotube $(m, 0)$, placed on a multilayer substrate and covered with a two-layer graphene sheet. Internal pressure distribution is shown by different colors, blue — zero pressure, red — maximum pressure P_{\max} . Parts (a–d) show the open state of a nanotube with $m = 5, 10, 20, 40$ ($P_{\max} = 9.7, 8.9, 2.8, 2.4$ GPa), part (e) shows the collapsed state of a nanotube $(40,0)$ ($P_{\max} = 5.5$ GPa).

layers in the covering sheet. Sheet covering of a nanotube causes the same effects as the external hydrostatic pressure. Effective (internal) pressure $P_{n,j}$ applied to particle n of chain j may be defined as a normal component of a force applied to this particle from other chains (force projection on the vector orthogonal to the chain) divided by the local chain pitch multiplied by Δy .

Internal pressure distribution in a multilayer system is shown in Figure 2 and 3. As can be seen in the figures, pressure is distributed in the system unevenly, for most of the system links it is close to zero, but on some cyclic chain links it may reach $P_{\max} = 8$ GPa. It is convenient here to determine the mean pressure applied to the whole encapsulated nanotube $(m, 0)$

$$P = \frac{1}{2m} \sum_{n=1}^{2m} P_{n,l_1+1}.$$

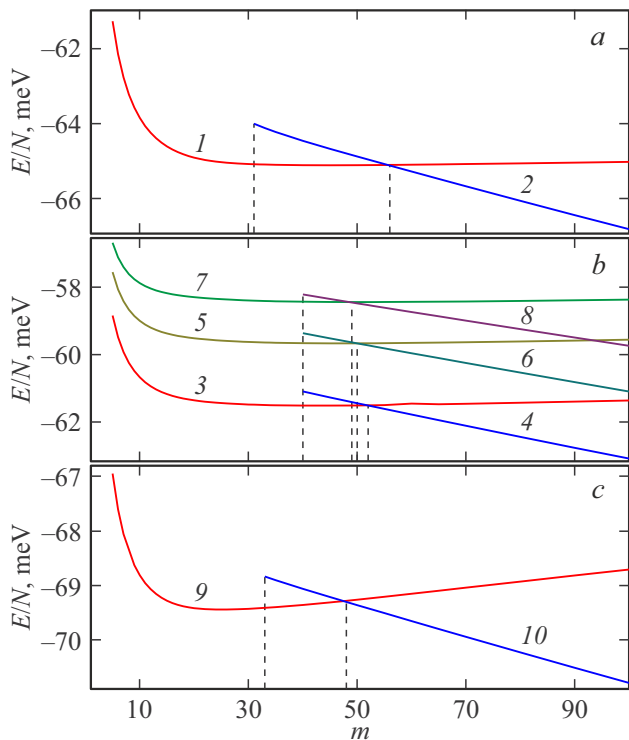


Figure 4. Dependence of the normalized energy E/N (N — the total number of particles) of the multilayer system with a carbon nanotube $(m, 0)$ on the chirality index m for a nanotube (a) lying on a multilayer substrate, b covered by a single-layer, two-layer and three-layer graphene sheet (curves 3, 4; 5, 6 and 7, 8), c covered with a h-BN sheet. Curves 1, 3, 5, 7, 9 give dependences for the open state and curves 2, 4, 6, 8, 10 give dependences for the collapsed nanotube state. The vertical dashed lines show the typical values of m_1 and m_2 .

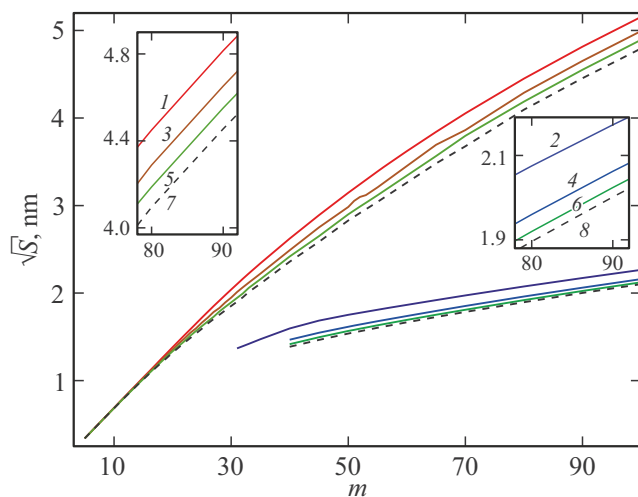


Figure 5. Dependence of the square root of cross-section area \sqrt{S} on the carbon nanotube index m for a nanotube lying on a multilayer flat substrate and covered with a l_3 -layer graphene sheet with $l_3 = 0; 1; 2$ and 3 (curves 1, 2; 3, 4; 5, 6 and 7, 8). Curves 1, 3, 5, 7 correspond to the open state and curves 2, 4, 6, 8 correspond to the collapsed state of a nanotube.

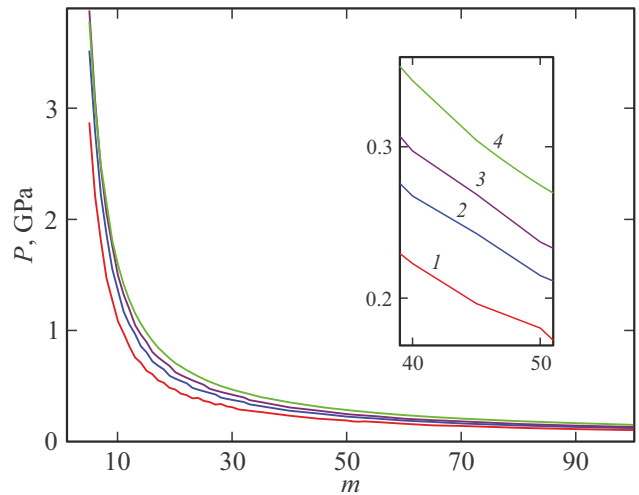


Figure 6. Dependence of the mean internal pressure P applied to the encapsulated carbon nanotube on m . Nanotube is in the open steady state. Curves 1, 2, 3 give the dependence for a nanotube covered by the l -layer graphene sheet ($l = 1, 2, 3$) and curve 4 gives the dependence for a nanotube covered with the h-BN sheet.

Dependence of P on m is shown in Figure 6, particular values are listed in Table 1. Internal pressure of the encapsulated nanotube decreases monotonously as m increases. Thus, at $m = 5, 10, 20, 40, 80, P = 2.87, 1.07, 0.46, 0.22, 0.11$ GPa for the single-layer cover. Twofold increase in the nanotube diameter causes more than twofold decrease in the internal pressure. Increase in the number of layers in the covering graphene sheet causes just a minor increase in the pressure. A higher pressure occurs when the nanotube is covered by the h-BN sheet, which is due to a stronger interchain interaction.

Let's consider how the pressure is distributed within the encapsulated nanotube cluster. For this, a molecular system with $l_2 > 1$ nanotubes $(5,0)$ covered with a single-layer graphene sheet is used (Figure 7). Steady states of the encapsulated cluster may be divided into single-layer and multilayer packings. In the single-layer packing, all nanotubes form a linear chain lying on a multilayer substrate (Figure 7, a, b, c), and in a multilayer packing, they form

Table 1. Compression coefficient k and mean internal pressure P for the carbon nanotube $(m, 0)$ covered with the l_3 -layer graphene sheet

m	k			P (GPa)		
	$l_3 = 1$	2	3	1	2	3
5	0.995	0.994	0.993	2.87	3.52	3.88
10	0.992	0.987	0.987	1.07	1.35	1.49
15	0.982	0.967	0.957	0.63	0.79	0.89
20	0.961	0.933	0.914	0.46	0.56	0.62
25	0.935	0.891	0.856	0.36	0.44	0.50
30	0.911	0.862	0.824	0.30	0.37	0.41
35	0.901	0.851	0.812	0.26	0.31	0.35

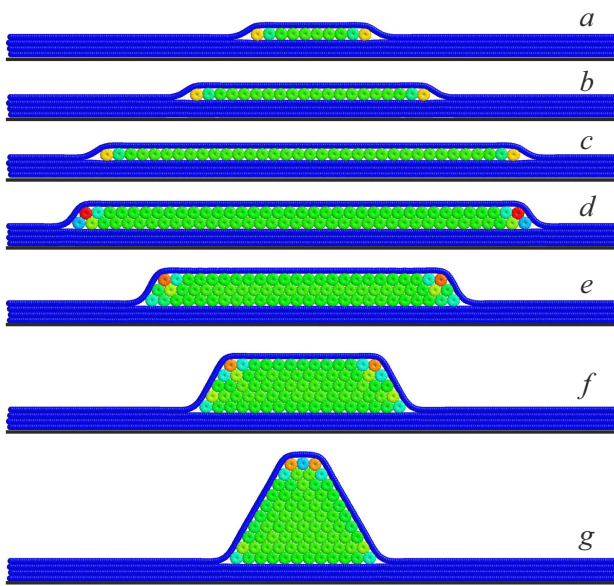


Figure 7. Stationary state of the k -layer packing consisting of l_2 nanotubes (5,0) covered by a graphene sheet with $k = 1$ and $l_2 = 10, 20, 35$ (a, b, c) and with $l_2 = 75, k = 2, 3, 5, 10$ (d, e, f, g). Distribution of internal pressure P over the nanotube cluster is shown by different colors, blue — zero pressure, red — maximum pressure $P_{max} = 3.55$ GPa.

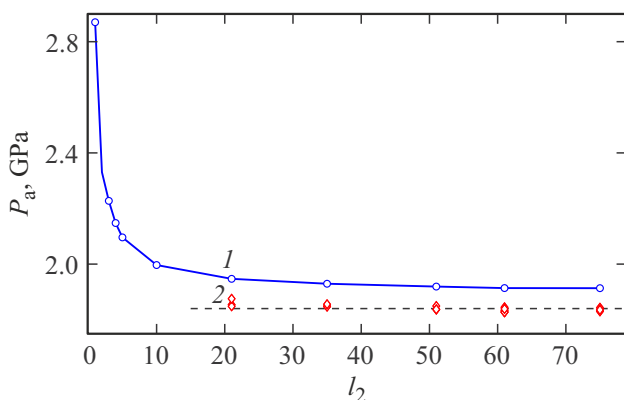


Figure 8. Dependence of the mean pressure P_a on the number of nanotubes l_2 in the encapsulated packing. Markers 1 show the dependence for a single-layer packing, markers 2 show the dependence for multilayer packings. Dashed line corresponds to $P = 1.84$ GPa.

a system of chains lying on each other, with their length decreasing monotonously from the lower to the upper layer (Figure 7, d, e, f, g).

Numerical solution of energy minimum problem (13) showed that the mean internal pressure in the nanotube cluster

$$P_a = \frac{1}{l_2} \sum_{j=1}^{l_2} P_j,$$

(P_j — pressure on the j -th nanotube) decreases monotonously as the number of nanotubes l_2 increase, but

when $l_2 > 50$, it approaches the threshold value (Figure 8). For the single-layer packing, this is $P_a \approx 1.91$ GPa, and for the multilayer packings (with the number of layers $k \geq 2$), this is $P_a \approx 1.84$ GPa. As shown in Figures 7, 12, pressure is distributed evenly within the cluster over all nanotubes — only end nanotubes in the single-layer packings and angular nanotubes in the upper layer of multilayer nanotubes are subjected to a higher pressure. Thus, the Pascal law is true for the encapsulated nanoparticle cluster for the internal pressure.

4. Interaction between encapsulated nanotubes

To determine the interaction energy of two encapsulated nanotube, a multilayer molecular system with $l_2 = 2$ nanotubes ($m, 0$) covered by a graphene sheet is used (Figure 9). We take the initial configuration of the multilayer system corresponding to two spaced far apart encapsulated nanotubes and solve energy minimum problem (13) numerically. We obtain a stationary state with two non-interacting encapsulated nanotubes (Figure 9, a). Energy of this state will be used as a zero level.

The distance between nanotubes R is defined as a distance between their centers of gravity. Then we move the nanotubes a little towards each other and solve problem (13) again with an additional condition that fixes the coordinates of two links of cyclic chains that are spaced farthest apart (thus the distance between nanotubes is fixed). By repeating

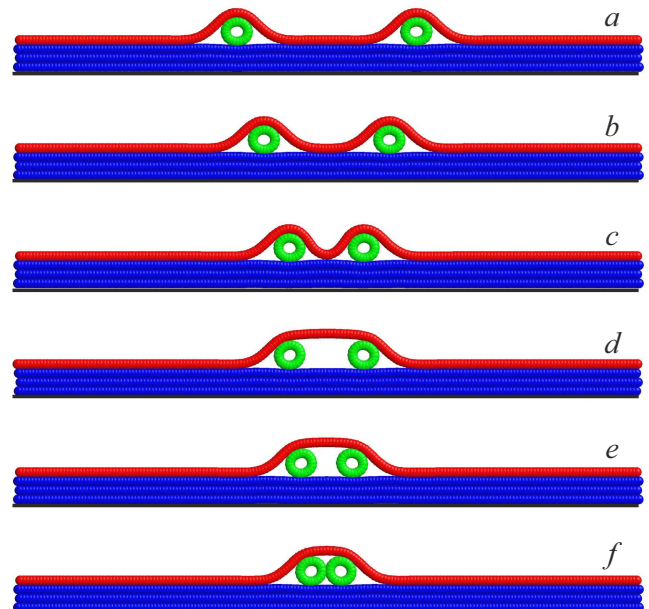


Figure 9. Steady states of the system consisting of two nanotubes (10,0) located on the multilayer substrate and covered with the top single-layer graphene sheet with the distance between centers $a - R = 6.65, b - 4.65, c - 2.76, d - 2.74, e - 1.90, f - 1.10$ nm. Blue — substrate sheets, green — nanotubes, red — top graphene sheet.

Table 2. Distances R_0 , R_1 , R_2 and energies E_0 , E_1 , E_2 for a pair of interacting nanotubes ($m, 0$) lying on a multilayer substrate without a cover ($l_3 = 0$) and with a single-layer graphene sheet cover ($l_3 = 1$)

$(m, 0)$	$l_3 = 0$		$l_3 = 1$			
	R_0 (Å)	E_0 (eV)	R_1 (Å)	E_1 (eV)	R_2 (Å)	E_2 (eV)
(5,0)	7.05	0.118	6.99	1.223	25.8	0.139
(8,0)	9.41	0.152	9.40	1.385	27.0	0.230
(10,0)	10.99	0.170	11.02	1.433	27.6	0.318

this procedure, the dependence of the system energy E on R is obtained. Dependence $E(R)$ of the interaction energy of two encapsulated nanotubes (covered with the single-layer graphene sheet) on the distance between them is shown in Figure 10.

When nanotubes lying on the multilayer substrate are not covered with a graphene sheet ($l_3 = 0$), then they interact as large Lennard–Jones particles. They form a bound state at a distance R_0 that is close to the Van der Waals diameter of the nanotube. $E(R)$ has a form of the Lennard–Jones potential with one minimum at $R = R_0$. Bond energy is $E_0 = -E(R_0) > 0$. When $R \nearrow +\infty$, $E(R) \nearrow 0$ as $-1/R^5$, when $R < R_0$ and $R \searrow 0$, $E(R) \nearrow +\infty$. Here, when $R < R_0$, nanotubes repel, and when $R > R_0$, nanotubes attract. Values for the equilibrium distance R_0 and bond energy E_0 for nanotubes with $m = 5, 8, 10$ are shown in Table 2.

If nanotubes are covered with a top graphene sheet ($l_3 = 1$), then the form of interaction varies. There is a critical distance R_2 , at which the type of interaction varies: when $R > R_2$, the nanotubes repel, and when $R < R_2$, the nanotubes attract. Repulsion of the encapsulated nanotubes at large distances is attributed to the behavior of the

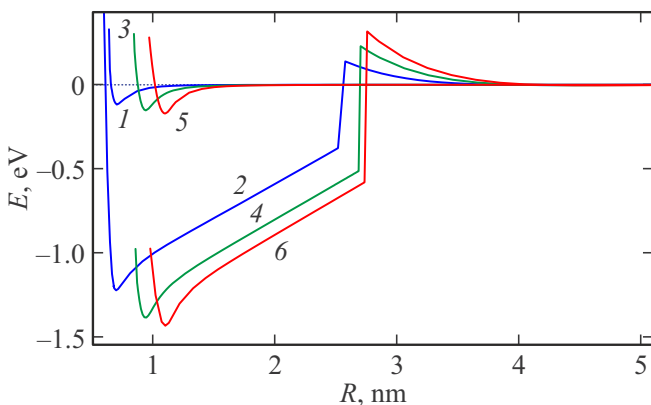


Figure 10. Dependence of E of two nanotubes lying on the multilayer substrate on the distance between their centers of gravity R . Curves 1, 2; 3, 4 and 5, 6 show the dependence for nanotubes (5,0); (8,0) and (10,0). Curves 1, 3, 5 show the dependence for uncovered nanotubes ($l_3 = 0$), curves 2, 4, 6 show the dependence for nanotubes covered with a single-layer graphene sheet ($l_3 = 1$).

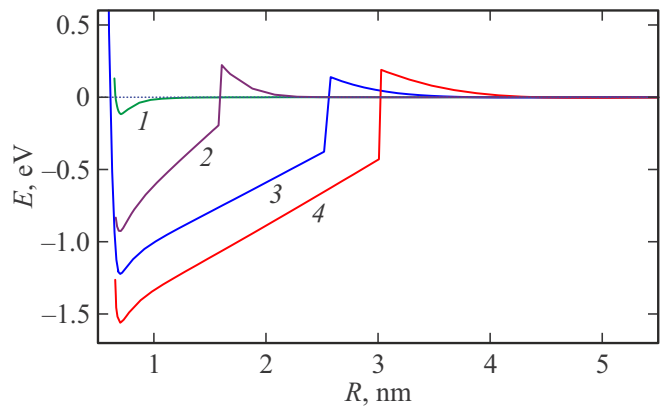


Figure 11. Dependence of E of two encapsulated nanotubes (5,0) on the distance between their centers of gravity R . Curve 1 give the dependence for uncovered nanotubes lying on the multilayer substrate ($l_3 = 0$), curve 2 — for nanotubes covered with the h-BN sheet, 3 and 4 — covered with single-layer ($l_3 = 1$) and two-layer ($l_3 = 2$) graphene sheet.

covering sheet in the area between them (Figure 9, *a, b, c*). Approaching of the nanotubes leads to reduced interaction between the covering sheet and multilayer substrate. The system energy increases monotonously at $R \searrow R_2$ and reaches its maximum $E_2 = E(R_2)$ at $R = R_2$. Then the sheet is separated from the substrate in the area between the nanotubes, thus, one two-particle encapsulation is formed. Further approach of the nanotubes causes monotonic decrease in energy to form a steady state at $R = R_1$ with the minimum energy $E(R_1) = -E_1$. Further approach of the nanotubes due to their repulsion leads to a quick energy growth. Therefore $E(R)$ for the encapsulated nanotubes has a form of a single-well potential with its minimum at $R = R_1$ and maximum at $R = R_2 > R_1$ (Figure 10). Values of R_1 , R_2 and E_1 , E_2 for nanotubes with $m = 5, 8, 10$ are shown in Table 2.

Behavior of $E(R)$ doesn't vary when the type of the covering sheet changes. $E(R)$ will have its maximum at $R = R_2$ for the multilayer graphene sheet and for the h-BN sheet. Only critical values of R_1 , R_2 and E_1 , E_2 will vary (Figure 11). Thus, merging of two encapsulations provides a considerable energy gain equal to E_1 , but their approach requires overcoming of an energy barrier with the height E_2 . Thus, for the encapsulated nanotubes (5,0), the gain from their mержence is $E_1 = 1.22$ (0.93 eV), and the energy barrier height preventing the mержence is $E_2 = 0.14$ (0.22 eV) when the covering G (h-BN) sheet is used. Therefore, mержence of such encapsulations may occur only at sufficiently high temperatures.

Nanotube encapsulation provides considerable increase in their interaction energy. The interaction energy of uncovered nanotubes (5,0) $E_0 = 0.12$ eV is ten times as low as the interaction energy of the encapsulated nanotubes $E_1 = 1.22$ eV.

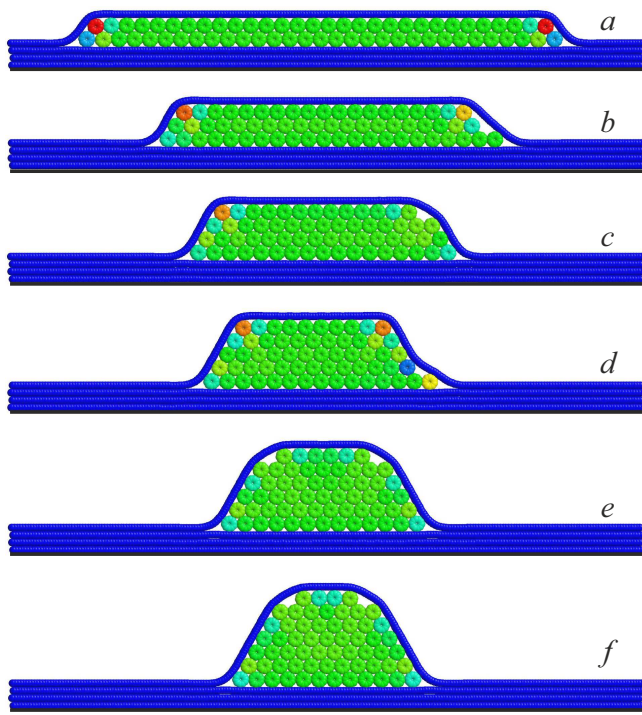


Figure 12. Steady k -layer packings consisting of $l_2 = 61$ nanotubes (5,0) covered with the single-layer graphene sheet at $a - k = 2$, $b - k = 3$, $c - k = 4$, $d - k = 5$, $e - k = 6$ and $f - k = 7$. Distribution of internal pressure P over the nanotube cluster is shown by different colors, blue — zero pressure, red — maximum pressure $P_{\max} = 3.56$ GPa.

5. Encapsulated cluster behavior

Let's consider the behavior of a nanotube cluster (5,0) placed on a flat multilayer substrate and covered with a top graphene sheet (Figure 12). For this, a substrate consisting of $l_1 = 3$ linear chains with periodic boundary conditions (number of links $N_s = 600$) is used. A cluster consisting of $l_2 = 61$ cyclic chains (the number of links $N_n = 10$) is placed compactly on the substrate and covered on top by a chain of $N_c = 580$ links ($l_3 = 1$). The nanotube cluster has 7 steady k -layer packings, $k = 1, \dots, 7$. A single-layer packing has the highest energy E_0 . This value will be used as a zero energy level, then the energy of a k -layer packing is $E_k - E_0 = 0, -2.47, -3.07, -3.45, -3.20, -3.41, -3.29$ eV with $k = 1, \dots, 7$. Packings with the number of layers $k = 4$ and 6 are most energetically favorable.

To simulate thermal vibrations, the molecular system is placed in a Langevin thermostat. Multilayer system behavior will be described by the Langevin system of equations.

$$M_1 \ddot{\mathbf{u}}_n = -\frac{\partial H}{\partial \mathbf{u}_n} - \Gamma M_1 \dot{\mathbf{u}}_n + \Xi_n, \quad n = 1, \dots, N, \quad (14)$$

where $N = l_1 N_s + l_2 N_n + l_3 N_c$ is the total number of particles, $\Gamma = 1/t_r$ is the friction coefficient (relaxation time

$t_r = 10$ ps), $\Xi_n = (\xi_{n,1}, \xi_{n,2})$ is the two-dimensional vector of normally distributed random forces normalized by the following conditions

$$\langle \xi_{n,i}(t_1) \xi_{k,j}(t_2) \rangle = 2M_1 \Gamma k_B T \delta_{nk} \delta_{ij} \delta(t_2 - t_1)$$

(T is the thermostat temperature, k_B is the Boltzmann constant). A steady k -layer packing of nanotubes with $k = 1, \dots, 7$ is taken as a starting condition.

Numerical integration of the system of equations of motion (14) showed that when a top cover (with $l_3 = 0$) is not available, all nanotube clusters on the flat substrate remain stable only at $T < 290$ K. At a higher temperature, the cluster is disintegrated with separation of some nanotubes from the substrate.

Covering of the cluster with a graphene sheet (transition into the encapsulated state) increases the cluster stability considerably. Let's consider how the area encompassing the nanocluster between the substrate and covering chain varies as the temperature increases

$$S = \frac{1}{2} \sum_{n=1}^{N_c-1} (z_{n,l} + z_{n+1,l} - 2z_0)(x_{n+1,l} - x_{n,l}), \quad (15)$$

where $l = l_1 + l_2 + 1$ is the chain No. corresponding to the top graphene sheet,

$$z_0 = \frac{1}{100} \sum_{n=1}^{50} (z_{n,l} + z_{N_c-50+n,l})$$

is the level corresponding to the cavity bottom, $\mathbf{u}_{n,l} = (x_{n,l}, z_{n,l})$ sets the coordinates of the n -th particle of the l -th chain. Area S defines the interlayer pocket volume encompassing the nanotube cluster.

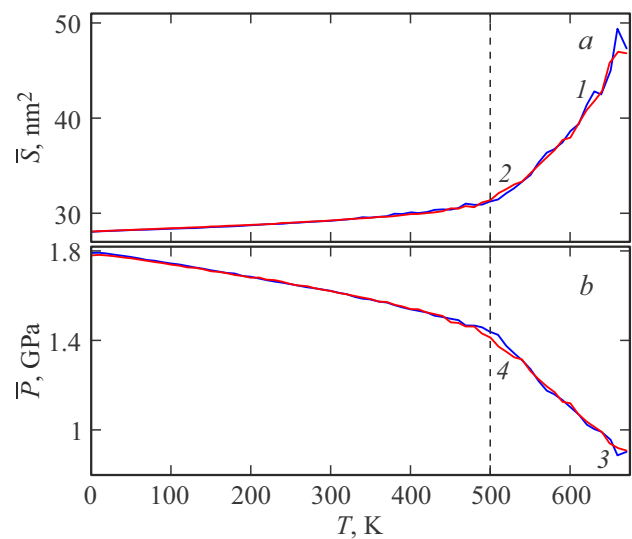


Figure 13. Dependence on T of a — the mean cavity area \bar{S} and b — the mean internal pressure in the cavity \bar{P} for the encapsulated cluster of $l_1 = 61$ nanotubes (5,0). Curves 1, 3 (blue) and 2, 4 (red) give the dependences for three-layer and six-layer clusters. Vertical straight line corresponds to $T = 500$ K.

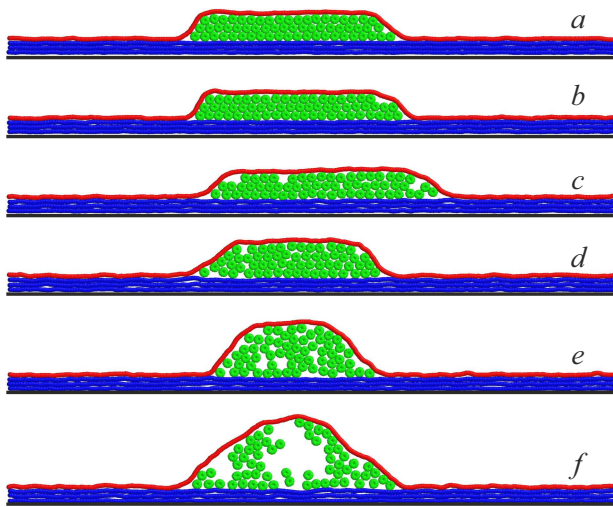


Figure 14. Configuration of the encapsulated cluster of $l_1 = 61$ nanotubes (5,0) at $a - T = 300$ K, $b - 400$ K, $c - 500$ K, $d - 530$ K, $e - 570$ K and $a - 670$ K. Blue — substrate sheets ($l_1 = 3$, $N_s = 600$), green — nanotubes ($N_n = 10$), red — top graphene sheet ($l_3 = 1$, $N_c = 580$). The cluster had a three-layer shape at the initial time.

Dependences of the mean area

$$\bar{S} = \lim_{t \rightarrow \infty} \frac{1}{t} \int_0^t S(\tau) d\tau,$$

and mean internal pressure

$$\bar{P} = \lim_{t \rightarrow \infty} \frac{1}{t} \int_0^t P_a(\tau) d\tau,$$

on T are shown in Figure 13. As shown in the figure, at $T < 500$ K, increase in the temperature causes gradual increase in the cavity area and related slow decrease in the internal pressure. The cluster structure in this case is retained (Figure 14, a, b). At $T = 500$ K, failure of the laminar cluster structure starts (Figure 14, c). Cluster melting starts and is followed by fast increase in the encapsulation cavity volume (Figure 14, d, e, f). Growth of \bar{S} increases dramatically and, therefore, \bar{P} decreases quickly. The cavity takes the shape of a semicircle. Note that full nanotube encapsulation is retained at all given temperatures $T < 700$ K. All nanotubes always remain within the local semicircle formed by the covering graphene sheet.

6. Conclusion

The numerical simulation showed that the encapsulation of nanotubes lying on a flat substrate (covering with graphene or hexagonal boron nitride sheet) facilitates nanotube collapsing (flattening). After encapsulation, the

collapsed state becomes more energetically favorable than the open state for nanotubes with $D > 3.75$ nm.

Covering of a nanotube with a sheet gives rise to an effective (internal) pressure on the nanotube surface that can reach its maximum values of 8 GPa in some areas. The mean internal pressure decreases monotonously with increasing nanotube diameter (twofold increase in the diameter leads to a more than twofold decrease in the pressure). Increase in the number of layers in the covering sheet causes just a minor increase in the pressure. A higher pressure occurs when a covering h-BN sheet is used.

During nanotube cluster encapsulation, the internal cluster pressure is distributed evenly. This suggests that the Pascal law is true within the encapsulated nanoparticle cluster for the internal pressure. For a nanotube cluster with the chirality index of (5,0), the internal pressure may reach 2 GPa.

Simulation of the interaction between two encapsulated nanotubes showed that they attract at small distances and repel at large distances. Nanotube encapsulation provides considerable increase in their interaction energy. Thus, the interaction energy of two uncovered nanotubes with the chirality index of (5,0) is ten times as low as the interaction energy of the encapsulated nanotubes. Merging of two encapsulations provides an energy gain of 1.22 eV, but their approach requires overcoming of an energy barrier of 0.14 eV. Therefore, mergence of individual encapsulations may occur only at sufficiently high temperatures.

Simulation of the nanotube cluster placed on a flat substrate shows that the cluster remains stable only at $T < 290$ K. At a higher temperature, the cluster is disintegrated, which is followed by separation of some nanotubes from the substrate. Covering of the cluster with a graphene sheet increases cluster stability. Here, the cluster retains its crystalline structure at $T < 500$ K, and melting occurs at a higher temperature followed by a quick increase in the interlayer cavity (pocket) volume encompassing the cluster. The cavity takes a form of semicircle, its volume increases monotonously with the temperature growth. At all given temperatures $T < 700$ K, all nanotubes are always within this cavity, i.e. their encapsulation is always maintained.

Funding

This study was carried out under the state assignment of the Federal Research Center for Chemical Physics Russian Academy of Sciences.

Conflict of interest

The authors declare no conflict of interest.

References

- [1] K.S. Novoselov, A.K. Geim, S.V. Morozov, D. Jiang, Y. Zhang, S.V. Dubonos, I.V. Grigorieva, A.A. Firsov. *Science* **306**, 5696, 666 (2004).

- [2] A.K. Geim, K.S. Novoselov. *Nat. Mater.* **6**, 3, 183 (2007).
- [3] C. Soldano, A. Mahmood, E. Dujardin. *Carbon* **48**, 8, 2127 (2010).
- [4] J.A. Baimova, B. Liu, S.V. Dmitriev, K. Zhou. *Phys. Status Solidi RRL* **8**, 4, 336 (2014).
- [5] J.A. Baimova, E.A. Korznikova, S.V. Dmitriev, B. Liu, K. Zhou. *Rev. Adv. Mater. Sci.* **39**, 69 (2014).
- [6] A.K. Geim. *Science* **324**, 5934, 1530 (2009).
- [7] C. Lee, X. Wei, J.W. Kysar, J. Hone. *Science* **321**, 5887, 385 (2008).
- [8] A.A. Balandin, S. Ghosh, W. Bao, I. Calizo, D. Teweldebrhan, F. Miao, C. N. Lau. *Nano Lett.* **8**, 3, 902 (2008).
- [9] Y. Liu, C. Hu, J. Huang, B.G. Sumpter, R. Qiao. *J. Chem. Phys.* **142**, 24, 244703 (2015).
- [10] A.K. Geim, I.V. Grigorieva. *Nature* **499**, 419 (2013).
- [11] L. Wang, I. Meric, P.Y. Huang, Q. Gao, Y. Gao, H. Tran, T. Taniguchi, K. Watanabe, L.M. Campos, D.A. Muller, J. Guo, P. Kim, J. Hone, K.L. Shepard, C.R. Dean. *Science* **342**, 614 (2013).
- [12] R. Xiang, T. Inoue, Y. Zheng, A. Kumamoto, Y. Qian, Y. Sato, M. Liu, D. Tang, D. Gokhale, J. Guo, K. Hisama, S. Yotsumoto, T. Ogamoto, H. Arai, Y. Kobayashi, H. Zhang, B. Hou, A. Anisimov, M. Maruyama, Y. Miyata, S. Okada, S. Chiashi, Y. Li, J. Kong, E.I. Kauppinen, Y. Ikuhara, K. Suenaga, S. Maruyama. *Science* **367**, 537 (2020).
- [13] Y. Zhang, C. Hu, B. Lyu, H. Li, Z. Ying, L. Wang, A. Deng, X. Luo, Q. Gao, J. Chen, J. Du, P. Shen, K. Watanabe, T. Taniguchi, J.-H. Kang, F. Wang, Y. Zhang, Z. Shi. *Nano Lett.* **20**, 2770 (2020).
- [14] K.S. Vasu, E. Prestat, J. Abraham, J. Dix, R.J. Kashtiban, J. Beheshtian, J. Sloan, P. Carbone, M. Neck-Amal, S.J. Haigh, A.K. Geim, R.R. Nair. *Science* **353**, 12168 (2016).
- [15] E. Khestanova, F. Guinea, L. Fumagalli, A.K. Geim, I.V. Grigorieva. *Nat. Commun.* **7**, 12587 (2016).
- [16] C. Hu, J. Chen, X. Zhou, Y. Xie, X. Huang, Z. Wu, S. Ma, Z. Zhang, K. Xu, N. Wan, Y. Zhang, Q. Liang, Z. Shi. *Nat. Commun.* **15**, 3486 (2024).
- [17] L. Zhang, Y. Wang, J. Lv, Y. Ma. *Nat. Rev. Mater.* **2**, 17005 (2017).
- [18] J. Zheng, X. Liu, P. Xu, P. Liu, Y. Zhao, J. Yang. *Int. J. Hydrogen Energy* **37**, 1, 1048 (2012).
- [19] N.G. Apkadirova, K.A. Krylova, J.A. Baimova. *Letters on Materials (Pisma o materialakh)* **12**, 4, 445 (2022). (in Russian).
- [20] A.V. Savin, E.A. Korznikova, S.V. Dmitriev. *Phys. Rev. B* **92**, 035412 (2015).
- [21] A.V. Savin, E.A. Korznikova, S.V. Dmitriev. *FTT* **57** 11, 2278 (2015).
- [22] A.V. Savin, E.A. Korznikova, S.V. Dmitriev. *Phys. Rev. B* **99**, 235411 (2019).
- [23] A.V. Savin. *ZhETF* **160**, 6, 885 (2021) (in Russian).
- [24] A.V. Savin, O.I. Savina. *FTT* **61**, 11, 2257 (2019). (in Russian).

Translated by E.IIinskaya